Materials and Structures/Matériaux et Constructions, 1989, **22**, 35–47

Steel-to-concrete bond after concrete splitting: test results

PIETRO G. GAMBAROVA
Department of Structural Engineering, Politecnico di Milano, Milan 20133, Italy
GIAN PAOLO ROSATI, BARBARA ZASSO
Civil Engineers, Novara 28100, Italy

The definite trend towards the use of large-diameter rebars and the introduction of high-strength steels (f_y = 500 to 600 MPa) make it necessary to study the effects of longitudinal splitting on the steel-to-concrete bond. The study of splitting effects requires firstly basic tests to be performed in order to gather experimental information on bond and confinement stresses acting at the bar-to-concrete interface. For this purpose, three series of tests were recently carried out at the Politecnico di Milano. The results make it possible to ascertain a few basic properties of the bond after concrete splitting, and to formulate empirical constitutive laws regarding the stresses and the displacements (bar slip and opening of the splitting crack). All specimens consisted of a short deformed bar embedded in a concrete block, which had a preformed splitting crack in the plane passing through the bar axis: twelve specimens (Tests A and C) were fitted up with a round deformed bar having crescent-shaped lugs (D_b = 18 mm); seven specimens (Tests B) were fitted up with a specially machined deformed bar having a rectangular cross-section and straight lugs, so that concrete deterioration close to the bar could be investigated at the surface of the specimen, by means of the moiré technique. The tests were carried out at constant slip rate, up to very large slip values ($\delta_{t_{max}}/D_b$ = 0.25 to 0.30); both the ascending and the descending branches of the stress–slip curves were measured, for four different values of the opening of the splitting crack. The agreement among the results of the three series is generally satisfactory and often very good: consequently, constitutive laws regarding the four main variables (crack opening and bar slip, shear and confinement stresses) can be worked out, as will be shown in a companion paper on constitutive relationships and on concrete deterioration at the bar-to-concrete interface.

NOTATION

D_b, E_s, f_y	Diameter, Young's modulus and yield stress of the reinforcing bar
D_b^*, E_s^*, f_y^*	Diameter, Young's modulus and yield stress of the confinement rods
f_c', f_{ct}	Concrete cylindrical strength in compression and in tension
f_R	Bond index of the reinforcing bar
L	Bonded length of the reinforcing bar
$N = N_i - N_s$	Confinement force
N_i, N_s	Confinement forces exerted by the lower rods (always in tension) and by the upper rods (always in compression except at the beginning of the loading process)
V	Force applied to the reinforcing bar
δ_n, δ_n°	Nominal opening and initial opening of the preformed splitting crack
δ_t, δ_t°	Bar slip and initial 'free' slip
$\delta_t^* = \delta_t - \delta_t^\circ$	Reduced bar slip (bond stress curves)
$\Delta\delta_t$	Confinement lag
σ	Confinement stress
τ	Bond stress

1. INTRODUCTION AND NATURE OF PROBLEM

The resistant mechanisms upon which the steel-to-concrete bond is based are already well known, due to the many test results that have been gathered and analysed in the last thirty years, by resorting to a variety of specimens and techniques (see for instance the literature review by Tassios [1]).

The scientists who have contributed to the knowledge of the many aspects of bonding agree that the interaction between the concrete and a bar subjected to a pull-out force is characterized by four different stages (Fig. 1):

Stage I: for small values of the bond stress, $\tau \leq (0.5 \text{ to } 0.8)f_{ct}$, bond efficiency is assured by chemical adhesion, and no bar slip occurs.

Stage II: for larger bond stress values, $\tau = (0.7 \text{ to } 1.5)f_{ct}$, the chemical adhesion breaks down, the lugs of the bar induce large bearing stresses in the concrete, transverse microcracks originate at the tips of the lugs allowing the bar to slip, but the wedging action of the lugs remains limited (bonding is assured by the so-called bearing action).

Stage III: for still larger values of τ, $\tau = (1 \text{ to } 3)f_{ct}$, the

0025-5432/89

first longitudinal cracks form as a result of the increasing wedging action of the lugs, which produces tensile hoop stresses in the surrounding concrete [2]: as a consequence, a confinement action is exerted by the concrete on the bars and the bond is assured by bar-to-concrete interlock.

Stage IV: once the longitudinal cracks (splitting cracks) break out through the whole cover and bar spacing, the bond fails abruptly if no transverse reinforcement is provided. On the other hand, a sufficient amount of transverse reinforcement (namely stirrups) would assure bond efficiency in spite of concrete splitting, because of the confinement action developed by the reinforcement. In Stage IV, bond stress values as large as (1/3 to 1/2) f'_c can be reached, with the unavoidable and often unacceptable side-effect represented by very large slip values ($\delta_t/D_b \geq 0.05$).

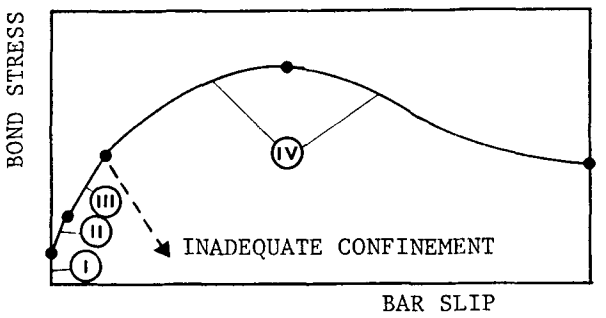

Fig. 1 Local bond–slip law.

At increasing slip values, the bond strength reaches a peak and then starts decreasing (Fig. 1), but still the bond strength remains remarkable even at very large slip values (τ = (0.15 to 0.30)f'_c for $\delta_t/D_b \geq 1/3$, in the case of round deformed bars with 18 mm diameter); in the end, bond behaviour tends to become of the dry-friction type (Coulomb type), since the concrete keys between the lugs are crushed or sheared off, and the tips of the lugs rub against the concrete without any appreciable increase of the wedging action.

In Fig. 2 the possible different bond situations along an anchorage (Fig. 2a) and a lapped splice (Fig. 2b) are sketched.

With regard to Stage III, due to the build-up of the wedging action exerted by the bars and to the propagation of splitting cracks, all possible contributions to confinement are mobilized: as a matter of fact, the confinement efficiency depends on the concrete cover and bar spacing [3–5,17], on transverse reinforcement [3,6–10,17,18] and on transverse pressure [11,12].

With regard to the ultimate strength of short anchorages and lapped splices subjected to a pull-out load, the simple behavioural model of Tepfers [2,13] gives a realistic prediction. According to this model, at the end of Stage III a cracked concrete sleeve forms around the bars, while an outer, solid sleeve – subjected to tensile

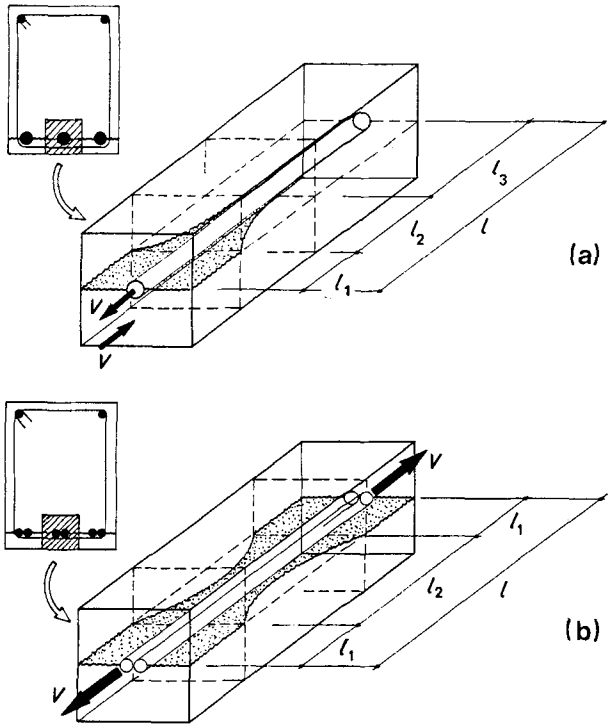

Fig. 2 Bond behaviour in (a) an anchorage and (b) a lapped splice: complete splitting in l_1, partial splitting in l_2, transverse cracking or chemical adhesion in l_3.

hoop stresses – exerts the confinement action necessary to prevent the bar from sliding out of the concrete mass (Fig. 3b). The bond fails once the thickness of the inner, cracked sleeve exceeds a critical value. Tepfer's partially cracked model represents a 'lower bound' with regard to bond strength, whilst perfect plasticity for the concrete (Fig. 3a) leads to an overestimation of the ultimate pull-out force (short bond lengths are considered here).

Stage III is certainly very common both in anchorages and in splices (thin longitudinal splitting cracks often appear along the bottom surface of beams in bending), in the working load situation as well as at collapse: for these reasons special attention has been devoted so far to Stage III, whilst Stage IV has been investigated far less, although the outbreak of splitting cracks through the entire concrete cover and bar spacing may lead to a fragile collapse, which can be prevented only by means of a careful design of the transverse reinforcement.

Thinking of transverse reinforcement, for instance in a beam subjected to bending and shear, in an anchorage or in a lapped splice (Figs 2 and 4), a proper design of the stirrups requires a knowledge of the constitutive laws $\tau(\delta_t,\delta_n)$ and $\sigma(\delta_t,\delta_n)$ or $\tau(\sigma,\delta_n)$ of Stage IV: for a given crack width W (the maximum bar slip $\delta_{t_{max}}$ is close to $W/2$, Fig. 4a) and a given bond stress (as required by the tensile force in the reinforcement), the curves for bond stress against bar slip make the evaluation of the splitting width δ_n possible (Fig. 4b). Then, by introducing the values of δ_n and τ into the bond–confinement curves, it is possible to evaluate the necessary confinement stress σ (Fig. 4c), and

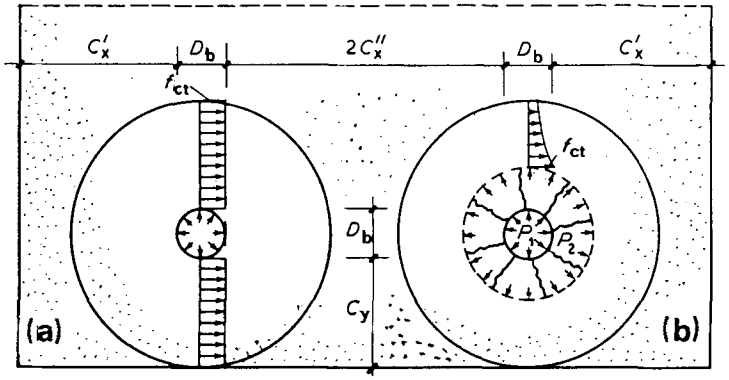

Fig. 3 Hoop stresses in the concrete according to (a) the plastic model and (b) the elasto-cracked model of Tepfers [2,13].

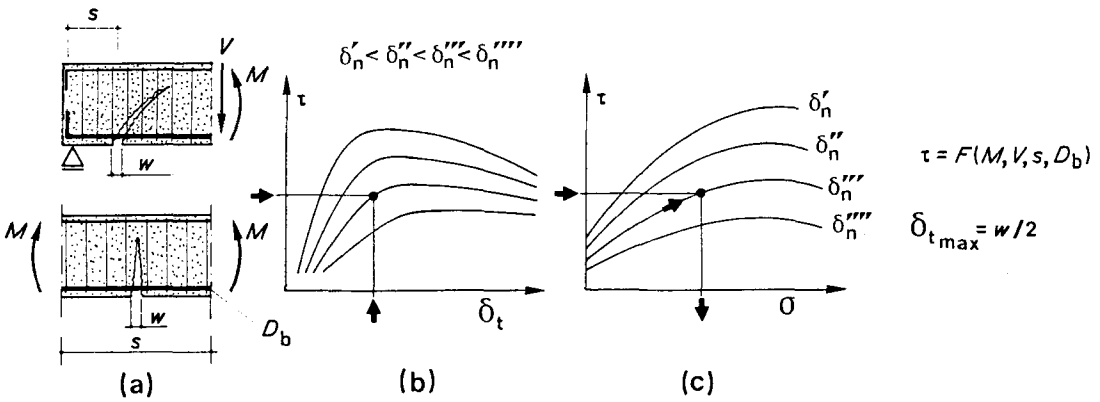

Fig. 4 (a) An anchorage or a beam subjected to bending, with possible use of (b) the local bond–slip law and (c) the bond–confinement envelopes for evaluating the confinement to be exerted by the stirrups.

to check whether the transverse reinforcement (stirrups) is adequate or not; alternatively, once the confinement stress is known, the amount of transverse reinforcement is easily found. Obviously such an approach for the analysis of bonding is justified in the case of sections with large steel ratios, high tensile stresses in the steel and closely spaced bars, since only by providing adequate confining steel can the bond strength be completely exploited.

Other reasons may explain the limited attention so far devoted to bond behaviour in Stage IV. A first reason is the widespread opinion that longitudinal splitting is dangerous both for bond strength and for structural durability, since bar corrosion may start from the longitudinal cracks. According to this point of view, longitudinal splitting should be prevented, being incompatible with structural safety in the working load situation, and with structural strength in the ultimate load situation (one of the major limit states could be prematurely activated because of longitudinal splitting and subsequent loss of bond). However, the test results so far obtained [14,15] and the further results presented in this paper show that bonding can be highly efficient even under serious longitudinal cracking, on condition that suitable confinement action is applied.

A second reason discouraging a widespread interest in bonding under severe splitting is that the actual code provisions do not consider explicitly the limit state of splitting; as a consequence, there are not sufficient stimuli for co-ordinated efforts on the subject.

As a matter of fact, the actual code provisions for concrete cover and bar spacing are generally on the safe side with regard to splitting (minimum 20 to 25 mm, and not less than one diameter), but past experience is mostly limited to small and medium bar diameters ($D_b < 30$ mm), to medium strength steels ($f_y < 400$ to 500 MPa) and to normal concretes. In these cases bond collapse is due to concrete crushing rather than to splitting, with the minimum transverse reinforcement specified by the codes.

With reference to splitting, the situation is even worse in lightweight concrete: since the cracks tend to spread through the aggregate particles, which no longer act as 'crack arrestors', the splitting cracks are more blunt and smooth. A somewhat similar situation is present also in high-strength concretes ($f'_c \geq 75$ MPa), where again the cracks spread across the aggregate particles because of the strong chemical bond between the aggregates and the mortar.

Within the above-mentioned framework, the purpose of this study is to present some systematic test results regarding bonding in a situation of complete concrete splitting, in order to work out, whenever possible, suitable constitutive relationships.

2. TEST PROGRAMME

The real problem of a bar embedded into a concrete mass with a splitting crack (Fig. 5a) has been drastically simplified (Fig. 5b) by adopting very simple specimens fitted with a single deformed bar (bonded length $L = 3D_b$), and having a preformed splitting crack, with smooth surfaces.

The specimens fall into two categories: Type 1 and Type 2 (Fig. 6), having practically the same bonded area and the same rib frontal section.

The test programme was carried out in three phases; the details of Phases A and B are given elsewhere [14,15] and will not be repeated here, whilst the test results will be referred to whenever necessary for the sake of comparison with the results of Phase C.

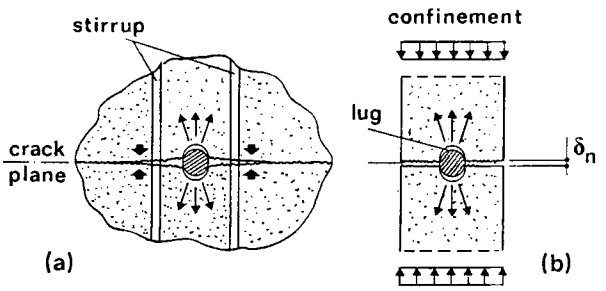

Fig. 5 Concrete splitting: (a) real situation and (b) possible modelling [14–16].

The specimens tested in Phase A and C are very similar (Type 1, Fig. 6a), the only difference being the thickness (50 and 90 mm, respectively). In both cases the reinforcement consists of a single round deformed bar, with 18 mm nominal diameter and crescent-shaped lugs (Fig. 7a): this kind of bar is very popular in Italy and is available in any diameter from 5 to 32 mm.

The specimens tested in Phase B are reinforced with a specially machined deformed bar, fitted with straight, constant-depth transverse lugs (Fig. 7b), having the same surface ratio (or bond index) as the round bars of Phase A and C ($f_R = 0.0602$).

The three phases were devised according to the following objectives:

Phases A and C: to gather test data on the stresses (bond and confinement) at the bar-to-concrete interface, at increasing bar slip and at constant opening of the preformed splitting crack: $\delta_t \leq (0.25 \text{ to } 0.30)D_b$, $\delta_n = 0.0$, 0.11, 0.22, 0.44 mm in Phase A, and $\delta_n = 0.0$, 0.10, 0.20, 0.30 mm in Phase C.

Phase B: to gather test data regarding the propagation and extension of the microcracked zone close to the bar: with the special bars used in Phase B and already described, the stress field close to the bar tends to be plane and the microcracked zone can be studied at the lateral surface of the specimen by means of the moiré technique (based on optical interferometry); the values adopted for the opening of the splitting crack were the same as in Phase A.

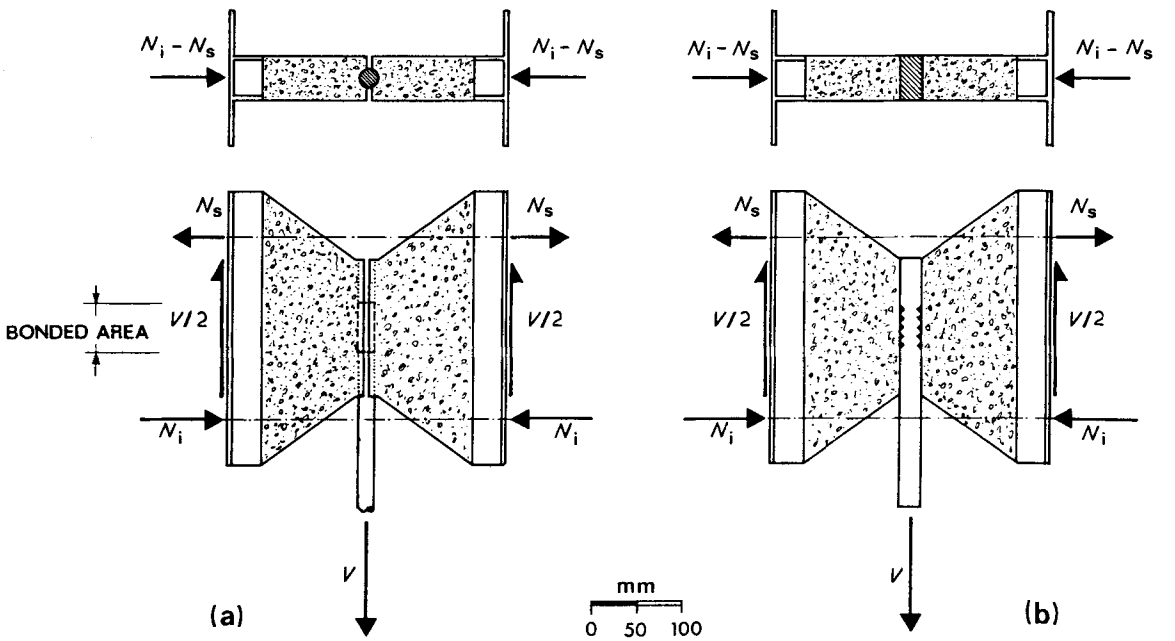

Fig. 6 Different specimens adopted in the analysis of bond behaviour after concrete splitting: (a) Type 1 [14,16] with a round deformed bar; (b) Type 2 [15] with a special bar having a rectangular cross-section.

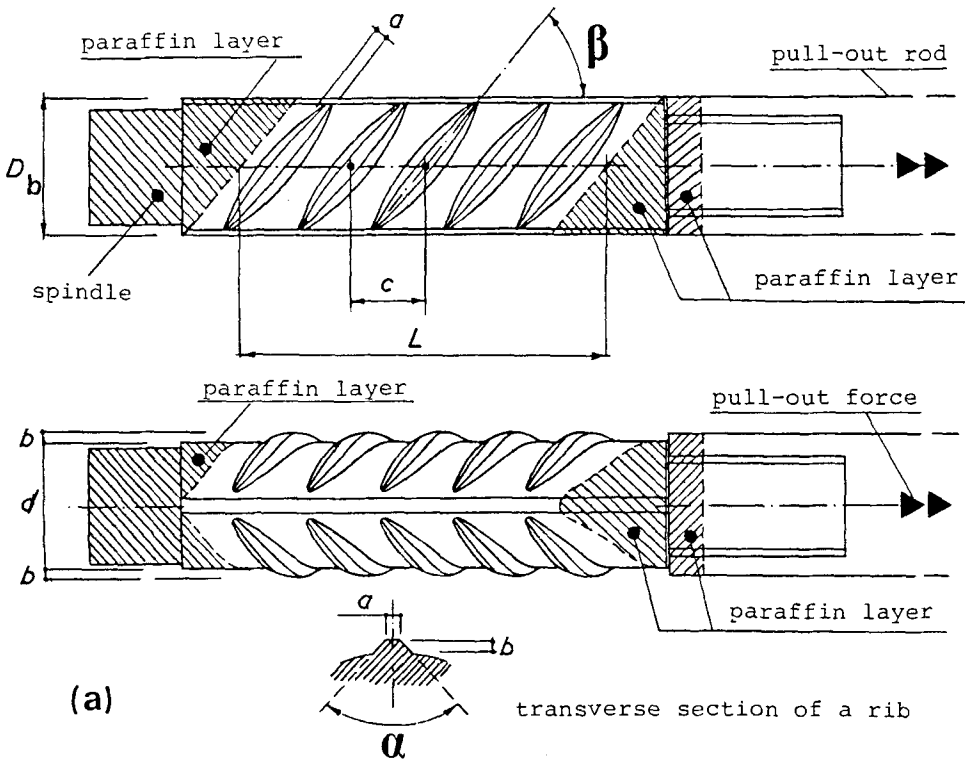

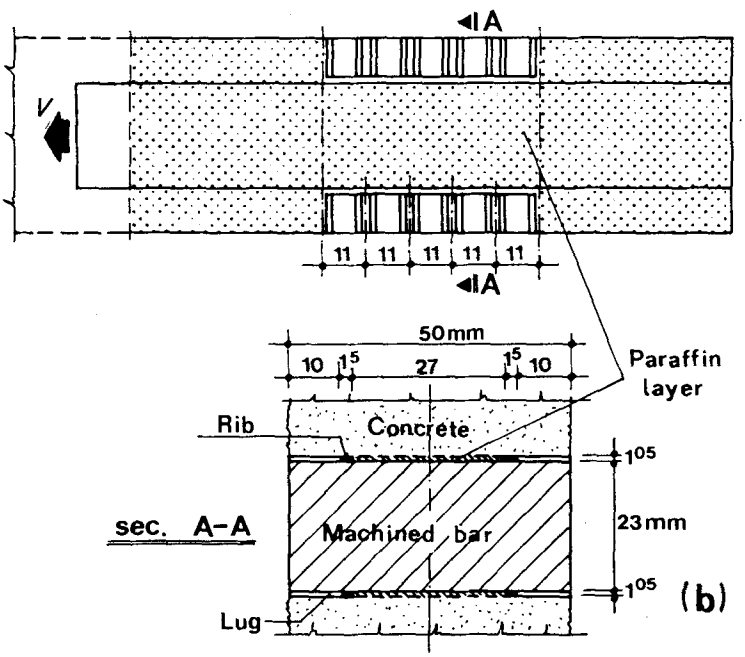

Fig. 7 Shape and dimensions of the deformed bars used in (a) Type 1 and (b) Type 2 specimens: D_b = 18 mm, d = 17.3 mm, L = 54 mm, a = 1.8 mm, b = 1.3 mm, c = 10.8 mm, α = 90°, β = 52°.

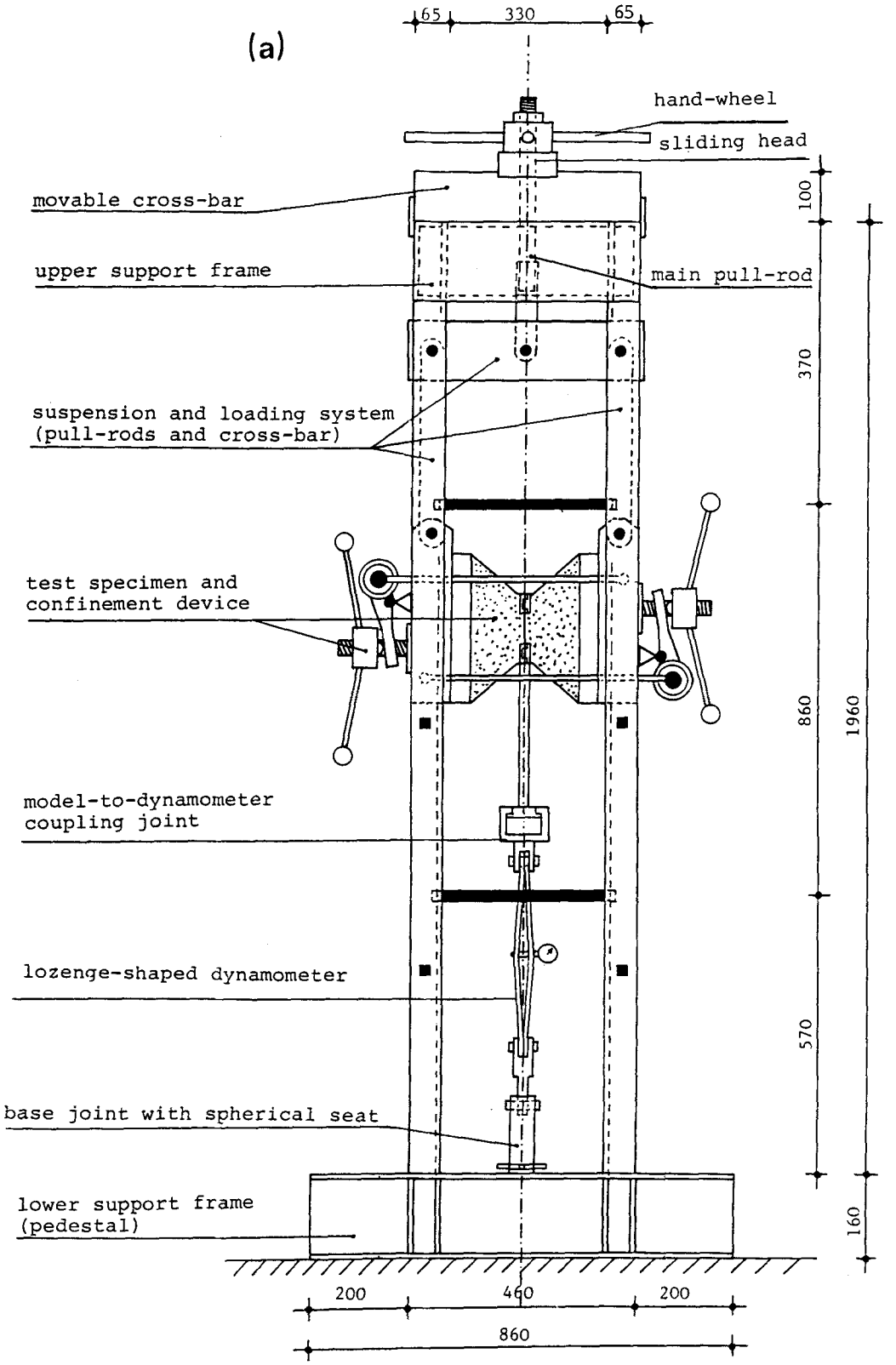

Fig. 8 Views of the mechanical testing machine and of the confinement device: (a) frontal view, (b) lateral view.

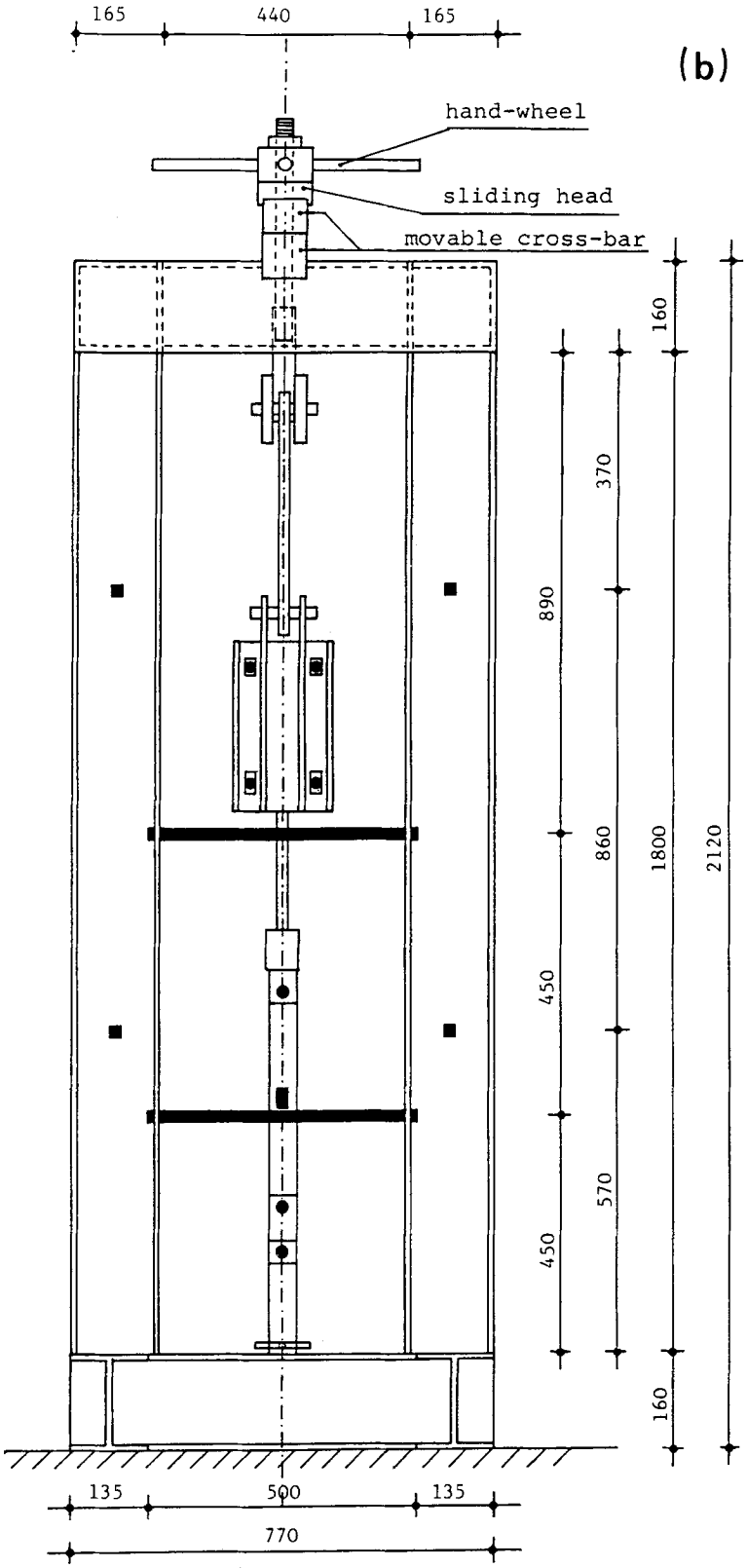
(b)
165
440
165
hand-wheel
sliding head
movable cross-bar
160
370
890
860
1800
2120
450
570
450
160
135
500
135
770

Fig. 8 Contd

In all, 22 concrete specimens were cast and 19 were successfully tested (four in Phase A, seven in Phase B and eight in Phase C). Three specimens were used partly for the calibration of the instruments and for the optimization of the loading process, partly to get accustomed to the unusual loading process. In Phase B, four out of seven specimens were tested with $\delta_n = 0.44$ mm, but in three cases (Tests 3, 4 and 5) the crack opening went out of control, and only the ascending branches of the stress–slip curves were measured. Only in Test 7 was the crack opening adequately controlled up to the very end of the test; for this reason, the linear branch of the curve shown below in Fig. 13b is the average of four tests.

The loading process was mostly stress-controlled in Phases A and B, with a back control on the displacements; in Phase C a very stiff mechanical testing machine was used (Fig. 8) and the displacements were adequately controlled.

In Phase A the unexpected and undesirable secondary splitting of the specimens in the mean plane (Fig. 13a below) made the results valid only for small values of the slip (full curves, Fig. 13a), because most of the ductility shown by the specimens is caused by the opening of the secondary splitting cracks; in Phase B the markedly less ductile behaviour of Type 2 specimens made it difficult to measure the descending branches of the stress–displacement curves (Fig. 13b below). Summing up, the results of the three phases are not always comparable, but – whenever they can be compared – the comparison is fairly good.

3. SPECIMEN CHARACTERISTICS, TEST PROCEDURE AND INSTRUMENTATION

Each specimen (Fig. 9) consists of two parts (also called blocks), which are in contact with the single reinforcing bar in a limited zone (five ribs, Fig. 7): the choice of the number of the ribs is a compromise between two con-

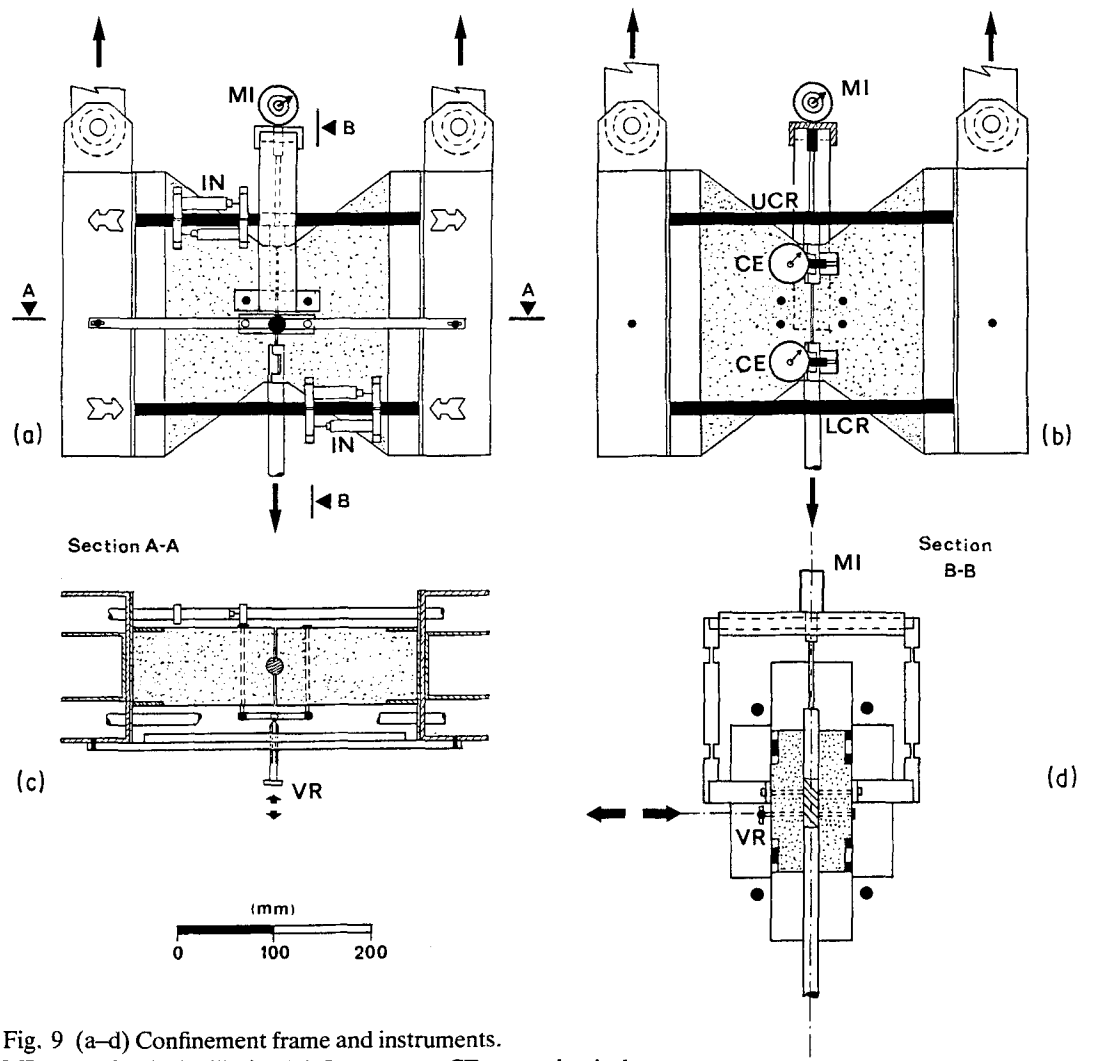

Fig. 9 (a–d) Confinement frame and instruments.
MI = mechanical millesimal deflectometer; CE = mechanical centesimal deflectometer; IN = pair of inductive millesimal deflectometers (Phase C, Series 2); VR = control screw for the reduction of possible out-of-plane displacements;
UCR = upper confinement rods; LCR = lower confinement rods.

flicting requirements (the analysis of local bond behaviour requires that the rib number is kept to a minimum, while the unavoidable lack of homogeneity of the concrete requires that at least a few ribs are engaged).

The splitting crack was preformed by inserting thin Plexiglas separators into the formwork, in the transverse plane passing through the bar axis. In this way, continuity between the blocks was prevented during concrete pouring; the separators were then removed after concrete hardening in order to let the confinement force be transferred from the blocks to the bar without any transmission by direct contact between the two blocks.

In the transverse plane of symmetry, besides the Plexiglas separators, steel keys were embedded in the concrete flush with the specimen faces (two keys for each face): these keys prevent differential slips between the two blocks, as would happen if, at increasing pull-out force, one block were to remain stuck to the bar, and the other block slipped. Then, because of the steel keys, the kinematic behaviour of the blocks is symmetric with respect to the bar (the keys do not affect the displacements of the two blocks at right-angles to the bar axis).

The reinforcing bar has five oblique ribs (Fig. 7a) and two barely protruding longitudinal ribs. The bar is threaded at one end, for the connection with the pull-out rod, and is machined at the other end in the shape of a smooth spindle, which protrudes from the specimen and is in contact with a millesimal deflectometer. The parts of the bar surface which are not supposed to be in contact with the concrete are covered by a thin layer of paraffin (1.5 to 2.5 mm). As a consequence, the bonded area (Fig. 6) is very well defined and the average of interface stresses can be correctly evaluated.

After concrete hardening, the wood and Plexiglas formwork of each specimen is removed and the specimen is fastened to a special confinement device which has four confinement rods (Figs 9b and d).

The confinement device is provided with levers and handwheels (Fig. 8a): the confinement rods have ball-and-socket joints at the ends, and also the lever supports are provided with ball-and-socket joints. Before starting each test, the confinement device and the specimen are fastened to the heads of a testing machine (maximum load 10^5N). A system of rods with ball-and-socket joints (Fig. 8) makes it possible to apply the pull-out force without undesirable side-effects.

The pull-out force is evaluated via a lozenge-shaped dynamometer which is very stiff axially, but is very sensitive to transverse bending: the displacements due to bending are measured by means of a millesimal deflectometer.

On average, each test required 5 to 6 days; slip values as large as 5 mm were measured; the number of loading steps was between 20 and 35, the average slip rate of the bar was kept very close to 0.05 mm h^{-1}, the confinement force was updated at least twice in each loading step, and the tolerance on the opening of the preformed crack was kept within $\pm$ 0.01 mm with respect to the prefixed value.

Because of the length of time required by each test, mechanical instruments were used to measure the displacements (Fig. 9). For the control of splitting width δ_n, four centesimal deflectometers were fastened to the steel keys (they measure the relative displacement of the two parts of each key). To measure bar slip, a millesimal deflectometer was fastened to the upper steel keys, by means of a suitable bridge-shaped attachment.

To measure the confinement, two of the four confinement rods were instrumented with a couple of mechanical deflectometers (specimens of Series 1) or inductive transducers (specimens of Series 2), all with 0.001 mm sensitivity. Possible out-of-plane displacements of the two blocks (which may rotate round the bar during the test) were reduced to zero by means of a screw (VR, Fig. 9) which could push or pull the two blocks; the screw was supported by a rod hinged to the lateral abutments.

The characteristics of the materials (concrete, steel of the reinforcing bars and steel of the confinement bars) are reported in the Appendix.

4. TEST RESULTS AND COMMENTS

As already mentioned, Phase C consists of eight specimens which were subjected to a pull-out test with four different values of the opening of the splitting crack: δ_n = 0.0, 0.1, 0.2, 0.3 mm. Consequently, two tests were performed for each value of δ_n. In two cases (Specimens 3 and 4 of Series 2: δ_n = 0.2 and 0.3 mm [16]) the initial value of the opening of the splitting crack turned out to be small but not nil, and had to be exactly evaluated (δ_n° = 0.094 mm, Specimen 3, and δ_n° = 0.050 mm, Specimen 4). The cause was probably concrete shrinkage.

As an example, the curves relating the pull-out force V and the confinement force N to slip are shown in Fig. 10 (Phase C, δ_n = 0.1 mm, Series 2): the values of V, N and δ_t (solid circles) are the so-called 'stabilized values' which correspond to a slip rate of less than 0.005 mm h^{-1}. As a matter of fact, in spite of the great stiffness of the test machine, each slip increase was followed by a further limited slip, because of the elastic deformations in the loading frame. This occurred only when the bond stress was close to the peak and just beyond the peak.

The stresses τ and σ were evaluated from the pull-out force V and the confinement force N, through the following self-explanatory equations:

$$\tau = \frac{V}{\pi D_b L} \qquad \sigma = \frac{2N}{\pi D_b L}$$

The average stress–displacement curves obtained in Phase C are shown in Fig. 11: the slip δ_t^* represents the bar slip corrected for the so-called 'free slip' δ_t° (see Fig. 14 below), which occurs during the opening of the splitting crack until the nominal value $\bar{\delta}_n$ is reached. The free slip δ_t° is related to rib shape and is almost a linear function of the nominal opening $\bar{\delta}_n$ ($\delta_t^\circ/D_b = 0.57\bar{\delta}_n/D_b$ in Phase C tests). In Phase A tests a limited but not negligible 'confinement lag' (Fig. 14) occurred [14], whilst this phenomenon was really negligible in Phase B and C tests [15, 16].

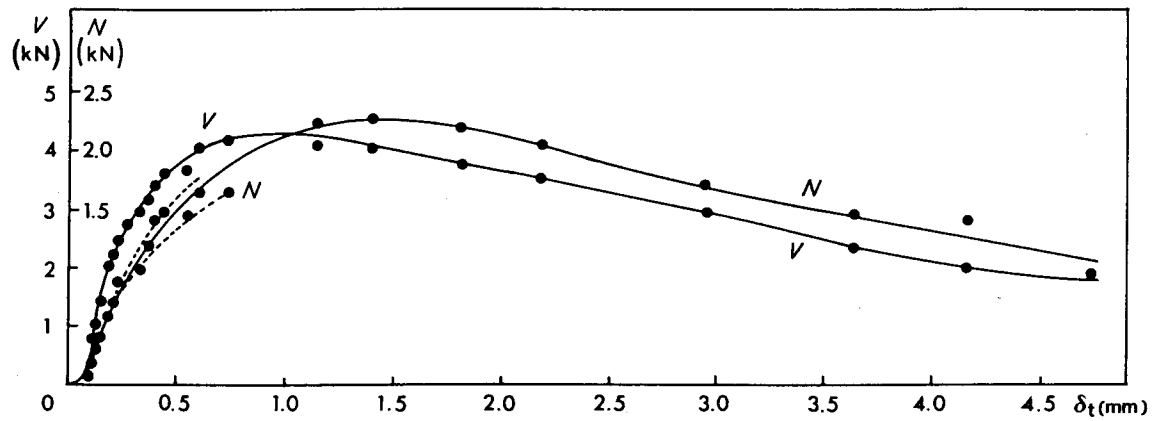

Fig. 10 Test results for $\delta_n = 0.1$ mm, Phase C, Series 2.

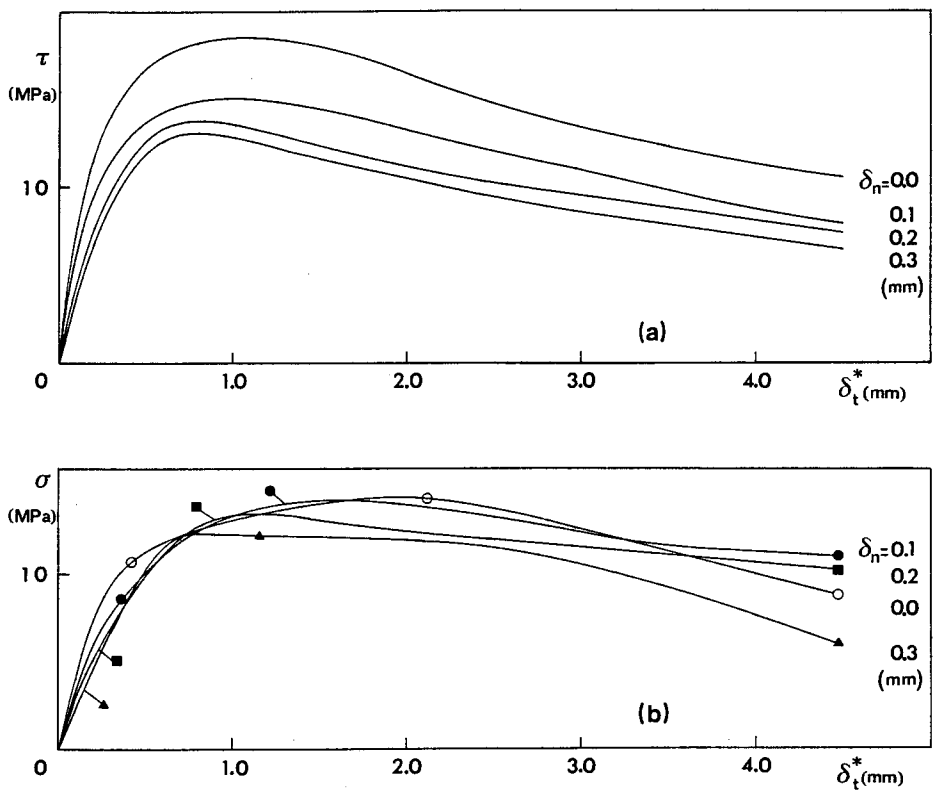

Fig. 11 (a) Bond and (b) confinement curves obtained from Phase C tests (average curves, Series 1 and 2). $f_c = 40.2$ MPa.

The bond–confinement envelopes of Phase C tests are plotted in Fig. 12 in a dimensionless form: if strain softening is disregarded, the envelopes reduce to a limited vertical first branch (cohesive behaviour), to a mostly linear second branch, followed by an almost flat third branch.

The stress–displacement curves of Phases A and B are shown in Figs 13a and b respectively. In Fig. 13a the dashed curves are affected by the secondary splitting: as a consequence, only the full curves are valid.

The tests performed in Phase B show that concrete deterioration due to microcracking at the bar-to-concrete interface is almost limited to a narrow band at either side of the bar, the band width being equal to maximum aggregate size. This localization of the damage within the concrete mass was also investigated by means of moiré grids attached to the back of each specimen: the results of this investigation are partly presented elsewhere [15], but further results and comments will be presented later in a paper regarding the constitutive relationships and concrete deterioration at the interface.

The three phases of the research project make it possible to ascertain a few interesting and important aspects of bond–splitting interaction:

(i) The bond strength (i.e. the peak value of the bond stress–slip curve) decreases at increasing values of the

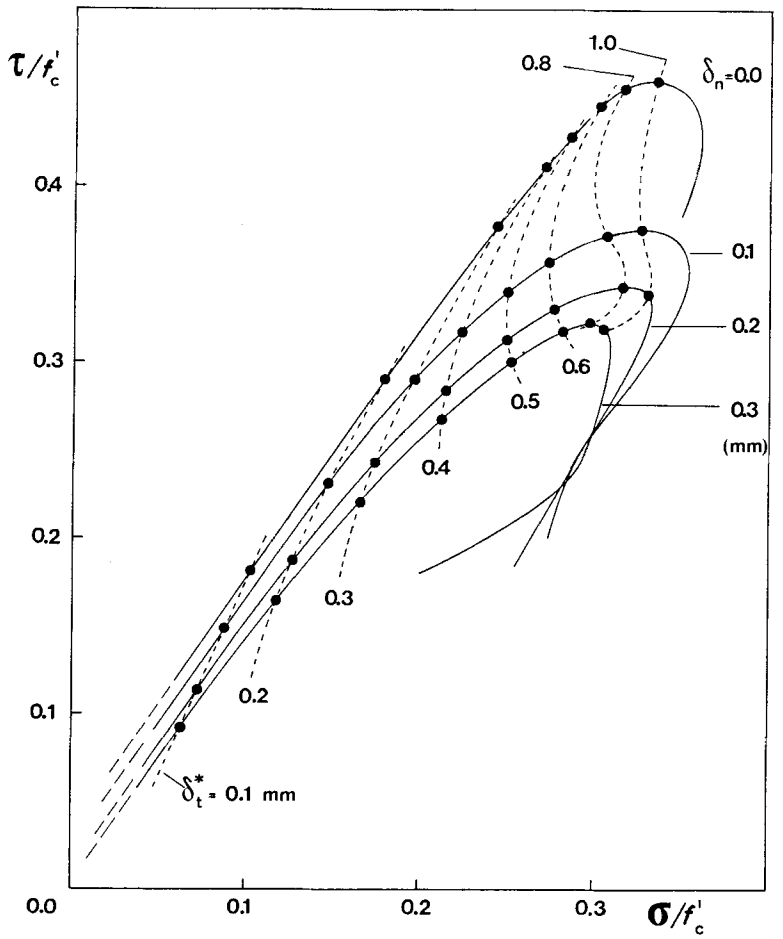

Fig. 12 Bond–confinement envelopes resulting from Phase C tests. f_c' = 40.2 MPa.

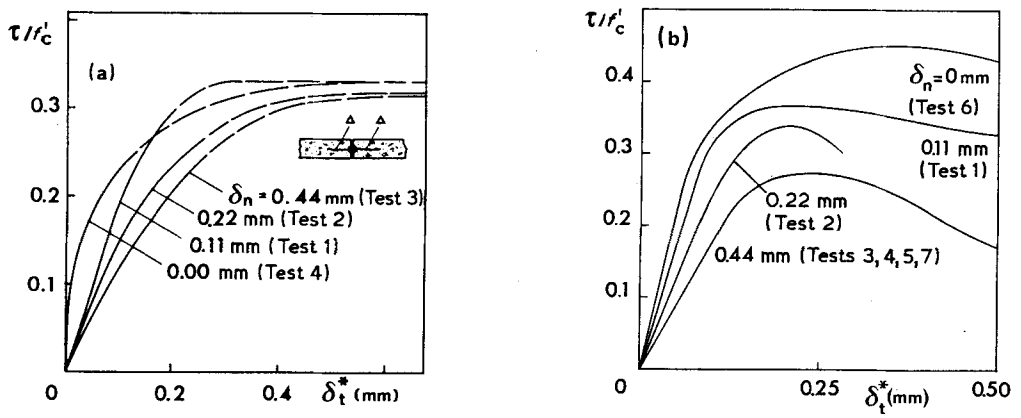

Fig. 13 Bond–slip curves resulting from tests. (a) Phase A: (---) after secondary splitting (Δ), f_c' = 32.8 MPa. (b) Phase B: f_c' = 37.5 MPa.

splitting crack opening, but is still close to 0.25 f_c' for crack openings close to 3% of the bar diameter (Figs 11a and 13b).

(ii) The peak value of the confinement stress is not strongly dependent on the opening of the splitting crack: the maximum confinement stress required to keep the width of the splitting crack at a prefixed value exhibits only a marginal decrease at increasing values of the crack opening (Fig. 11b).

(iii) Bond stiffness, $\partial\tau/\partial\delta_t^*$, decreases markedly at increasing values of the splitting crack opening (Figs 11a, 13a and 13b).

(iv) The bond–confinement envelopes, $\tau(\sigma)$, are basically linear for small and medium slip values

($\delta_t^*/D_b \leq 3\%$); for larger slip values, the envelopes flatten off; as a result, a tri-linear idealization seems reasonable, with a first, very limited branch characterized by cohesive behaviour, a second linear branch which becomes less and less steep at increasing crack width, and a third flat branch limited to $\sigma_n = (0.30 \text{ to } 0.35) f_c'$ (Fig. 12).

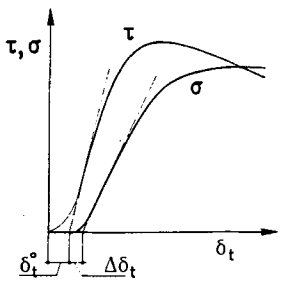

Fig. 14 Free slip δ_t° and confinement lag $\Delta\delta_t$: (——) $\delta_n = \bar{\delta}_n$, (——) $0 \leq \delta_n \leq \bar{\delta}_n$.

5. CONCLUSIONS

The formation of longitudinal cracks (splitting cracks) at relatively low values of the average bond stress makes bond behaviour rather sensitive to the confinement action exerted by the structural restraints or by transverse reinforcement. In order to prevent the limit state of bond loss (which is basically a local limit state) from preceding and thus favouring the most unfavourable of the principal limit states, a careful sizing of the transverse reinforcement is necessary, and in turn a clear understanding of how splitting cracks affect bond behaviour is required. To this end, test data on bond behaviour at different confinement levels or at different values of the splitting crack opening must be produced: this is the very scope of the research programme upon which this paper is based.

The tests were performed at different values of the opening of the preformed splitting crack, and the concrete specimens were reinforced with a single deformed bar ($D_b = 18$ mm, Type 6) having a three-diameter embedment length.

The good agreement between the three phases of this research project makes it possible to ascertain to what an extent the opening of the splitting crack affects the curves of bond stress against bar slip and the bond–confinement envelopes: as expected, at increasing crack width both the stiffness and the strength of the bond mechanism decrease, but still remain at an acceptable level, at least within the range of the values here considered for crack opening ($\delta_n/D_b < 2.5$ to 3%).

ACKNOWLEDGEMENTS

The work presented here was partly supported in the years 1983 to 1985 under grants given by the Italian Ministry for Higher Education (MPI) to the Politecnico di Milano, within the financial plan for research projects having national relevance (MPI 40%).

APPENDIX: Characteristics of the materials

Concrete

Standard compressive strength (3 cylinders, 100 mm diameter)	$f_c' = 35.8\ (44.5)$ MPa
Tensile strength (3 cylinders)	$f_{ct} = 3.65\ (4.50)$ MPa
Slump and water/cement ratio	75 mm, 0.65
Maximum aggregate size	15 mm
Portland cement content	332 kg m^{-3}
Casting direction: opposed to the pull-out force	
Age at the beginning of each series of tests	120 (210) days

The values between brackets refer to Series 2 of the tests.

Reinforcement bars

Cold-drawn ribbed bars made of medium-strength carbon steel, Type FeB 44 (Italian Building Code)

Yield stress	$f_y = 430$ MPa
Nominal diameter	$D_b = 18$ mm

Confinement rods:

Yield stress	$f_y^* = 710$ MPa
Young's modulus	$E_s^* = 191\,100$ MPa
Diameter	$D_b^* = 16$ mm

The rods were machined from round bars and threaded at the ends for the connection to the ball-and-socket joints: during the tests, the lower rods (LCR, Fig. 9b) were always in tension, whilst the upper rods (UCR, Fig. 9b) were always in compression, except at the beginning of the loading process, when a negative confinement force had to be applied in order to compel the preformed splitting crack to open up to the prefixed value.

REFERENCES

1. Tassios, T. P., 'Properties of bond between concrete and steel under load cycles idealizing seismic actions,' in Proceedings of AICAP–CEB Symposium, Rome, Avril 1979, CEB Bulletin No. 131, Paris, pp. 67–122.
2. Tepfers, R., 'Cracking of concrete cover along anchored deformed reinforcing bars,' *Mag. Concr. Res.* **31** (106) (1979) 3–12.
3. Ferguson, P. M., 'Bond stress: the state of art,' Report by ACI Committee 408, *ACI J. Proc.* **63** (11) (1966) 408.1 – 408.22.
4. Edwards, A. D. and Yannopoulus, P. J., 'Local bond stress–slip relationship under repeated loading,' *Mag. Concr. Res.* **30** (103) (1978) 62–72.
5. Ferguson, P. M., Turpin, R. D. and Thompson, J. N., 'Minimum bar spacing as a function of bond and shear strength,' *ACI J. Proc.* **50** (10) (1954) 869–888.
6. Chinn, J., Ferguson, P. M. and Thompson, J. N., 'Lapped splices in reinforced concrete beams,' *ibid.* **52** (15) (1955) 201–213.
7. Orangun, C. O., Jirsa, J. O. and Breen, J. E., 'Re-evaluation of test data on development length and splices,' *ibid.* **74** (3) (1977) 114–122.
8. Losberg, A. and Olsson, P. A., 'Bond failure of deformed reinforcing bars based on the longitudinal splitting effect of the bars,' *ibid.* **76** (1) (1979) 5–18.

9. Kemp, E. L. and Wilhelm, W. J., 'Investigation of the parameters influencing bond cracking,' *ibid.* **76** (1) (1979) 47–71.
10. Skorogobatov, S. M. and Edwards, A. D., 'The influence of the geometry of deformed steel bars on their bond strength in concrete,' *Proc. Instn Civil Engrs, Part 2* **67** (1979) 327–339.
11. Dörr, K., 'Bond-behaviour of ribbed reinforcement under transversal pressure,' in Proceedings of IASS Symposium on Nonlinear Behaviour of Reinforced Concrete Spatial Structures, Darmstadt, July 1978, Vol. 1, edited by G. Mehlhorn, H. Rühle and W. Zerna, Werner-Verlag, Düsseldorf pp. 13–24.
12. Robins, P. J. and Standish, I. G., 'The influence of lateral pressure upon anchorage bond,' *Mag. Concr. Res.* **36** (129) (1984) 195–202.
13. Tepfers, R., 'Lapped tensile reinforcement splices,' *J. Struct. Div. ASCE* **108** (ST1, Proc. Paper 16823) (1982) 283–301.
14. Gambarova, P. G. and Karakoç, C., 'Shear–confinement interaction at the bar-to-concrete interface,' in 'Bond in Concrete,' edited by P. Bartos (Applied Science, London, 1982), pp. 82–96.
15. Gambarova, P. G. and Chiamulera, G. B., 'Test results concerning the confinement effects on steel-to-concrete bond, after concrete splitting along the reinforcing bars,' in 'Studi e Ricerche,' Vol. 5, edited by S. Dei Poli (Politecnico di Milano, Milan, 1983) pp. 47–89 (in Italian).
16. Gambarova, P. G. and Zasso, B., 'The effects of cover splitting on steel-to-concrete bond: a review of some recent test results obtained at the University of Technology of Milan,' in 'Studi e Ricerche,' Vol. 7, edited by S. Dei Poli (Politecnico di Milano, Milan, 1985), pp. 7–54 (in Italian).
17. Morita, S. and Kaku, T., 'Splitting bond failures of large deformed reinforcing bars,' *ACI J. Proc.* **76** (1) (1979) 93–110.
18. Morita, S. and Fujii, S., 'Bond capacity of deformed bars due to splitting of surrounding concrete,' in 'Bond in Concrete,' edited by P. Bartos (Applied Science, London, 1982), 331–341.